UNLIMITED DISTRIBUTION

National Defence
Research and Development Branch

Défense nationale
Bureau de recherche et développement

TECHNICAL MEMORANDUM 95/215
May 1995

SOURCE LEVEL CALIBRATION OF THE DREA MOVING COIL PROJECTOR

John C. Osler — David M.F. Chapman

Defence Research Establishment Atlantic

Centre de Recherches pour la Défense Atlantique

DEFENSIO PER SCIENTIAM

Canada

National Defence
Research and Development Branch

Défense nationale
Bureau de recherche et développement

SOURCE LEVEL CALIBRATION OF THE DREA MOVING COIL PROJECTOR

John C. Osler — David M.F. Chapman

May 1995

Approved by C.W. Bright
Research Manager / Underwater Warfare

Distribution Approved by C.W. Bright

Research Manager / Underwater Warfare

TECHNICAL MEMORANDUM 95/215

Defence Research Establishment Atlantic

Centre de Recherches pour la Défense Atlantique

DEFENSIO PER SCIENTIAM

Canada

Abstract

The Defence Research Establishment Atlantic moving coil projector (MCP) generates acoustic power at low frequencies (below 250 Hz) by displacing water with two pistons which oscillate in phase. The source level of the MCP must be continually monitored because it varies in accordance with the operating state of the projector. Source level as a function of time may be determined by combining measurements of the acceleration of the forward and aft pistons in an appropriate manner. This document establishes the methodology to use in this process by comparing at-sea measured transmission loss of CW signals to theoretical calculations. This comparison reveals that corrections are required to the source level derived from the MCP accelerometers at the higher end of its frequency range.

Résumé

Le projecteur à bobine mobile (MCP) du Centre de reserches pour la défense Atlantique produit une puissance acoustique à basses fréquences (moins de 250 Hz) en déplaçant de l'eau avec deux pistons qui oscillent en phase. Le niveau d'émission doit être continuellement surveillé parce qu'il varie en fonction du mode de fonctionnement du projecteur. On peut déterminer le niveau d'émission en fonction du temps en combinant les mesures de l'accélération des pistons avant et arrière de facon appropriée. Ce document établit la méthodologie à utiliser dans ce processus en comparant la perte de transmission de signaux à ondes entretenues mesurée en mer aux calculs théoriques. Cette comparison révèle que des corrections sont nécessaires au niveau d'émission obtenu à partir des accéléromètres du MCP à l'extrémité supérieure de sa plage de fréquences.

Table of Contents

Section	Page
Abstract	ii
Resume	ii
Table of Contents	iii
List of Figures	iv
List of Tables	v
1. Introduction	1
2. Experimental Transmission Loss	2
Sea Trial	2
Data Analysis	3
Combining Acceleration of the Forward and Aft Pistons to Obtain Source Level	5
Inter-Piston Phase Differences and Projector Directionality	7
Received Level on Sonobuoys	8
Transmission Loss	9
3. Theoretical Transmission Loss	9
Geometry	10
Lloyd's Mirror Transmission Loss Calculations	12
Validation of Lloyd's Mirror Transmission Loss Model	13
4. Results	15
5. Conclusions and Recommendations	21
References	22
Appendix A: Source Level and Inter-Piston Phase	23
Appendix B: Comparison of TL Calculated using SAFARI and LM	26

List of Figures

Figure		Page
1.	Photograph of the DREA moving coil projector (MCP).	1
2.	Schematic of the steps followed in calibrating the MCP.	2
3.	Analysis flowchart	4
4.	The 41 Hz source level of the DREA MCP as a function of time.	6
5.	Received level on three sonobuoys deployed during the calibration of the MCP.	8
6.	Transmission Loss at 41 Hz as a function of time for the two sonobuoys used as receivers in the calibration of the MCP.	10
7.	Geometry of the source and receiver in the calibration of the MCP.	11
8.	Slant-range from the MCP to the receiving sonobuoys.	12
9.	The sound speed profile at the calibration site.	14
10.	TL vs. range according to SAFARI and Lloyd's mirror, between a 41 Hz source at 28.6 m depth and a receiver at 246.7 m depth.	15
11a.	Experimental Transmission Loss measurements on the Omni buoy overlain by the theoretical Transmission Loss at 4, 7, and 12.5 Hz.	16
11b.	Experimental Transmission Loss measurements on the Omni buoy overlain by the theoretical Transmission Loss at 22.5, 41, and 72 Hz.	17
12a.	Experimental Transmission Loss measurements on the VLA buoy overlain by the theoretical Transmission Loss at 4, 7, and 12.5 Hz.	18
12b.	Experimental Transmission Loss measurements on the VLA buoy overlain by the theoretical Transmission Loss at 22.5, 41, and 72 Hz.	19
A1.	Source level of the DREA MCP at 4, 7, 12.5, 22.5, 41, 72, and 225 Hz derived from accelerometers mounted on the forward and aft pistons.	23

A2. Phase angle between the accelerometers mounted on the forward and aft pistons of the DREA MCP at 4, 7, 12.5, 22.5, 41, 72, and 225 Hz. 25

B1. TL vs. range according to SAFARI and Lloyd's mirror between a source at 28.6 m depth and a receiver at 246.7 m depth: 4 and 7 Hz. 26

B2. TL vs. range according to SAFARI and Lloyd's mirror between a source at 28.6 m depth and a receiver at 246.7 m depth: 12.5 and 22.5 Hz. 27

B3. TL vs. range according to SAFARI and Lloyd's mirror between a source at 28.6 m depth and a receiver at 246.7 m depth: 41 and 72 Hz. 28

List of Tables

Table Page

1. Nominal source level and frequency of tones projected by the MCP. 3

2. Frequency windows for the signal and for upper and lower noise estimates which are applied when tracking narrowband lines and their signal level with PROPWR. 4

3. Theoretical maximum and measured phase differences between the fore and aft MCP pistons at all projected frequencies. 7

4. Parameters of Projector CPA on two Sonobuoys. 12

5. Corrections to the source level of the MCP as determined from combining signals from accelerometers mounted on the forward and aft pistons. 20

1. Introduction

The Defence Research Establishment Atlantic (DREA) moving coil projector (MCP), illustrated in Figure 1, is the principle acoustic source used in low frequency (below 250 Hz) environmental acoustic and detection experiments at DREA. There have been repeated observations that the source level of the MCP varies with time, differing from the nominal requested source level, in accordance with the operating state of the projector (*e.g.*. differential pressure[1]). Differential pressure may change as the projector moves up or down in the water column due to variations in tow ship speed and course or when the hydrostatic head is variable, as in rougher seas. Source level may also vary due to hydrodynamic effects, as the turbulent flow around the projector exerts an unsteady force on the piston face.

As the operating state is dynamic and there is currently no feedback loop that controls the MCP operating state to maintain a constant source level, it is necessary to monitor the source level as a function of time. When measurements of the acceleration of the forward and aft pistons are combined in an appropriate manner (Eq. 4), the actual source level of the MCP may be determined. To establish this methodology, a calibration experiment was conducted during sea-trial Q211 and the results are contained herein. The calibration is achieved by comparing the measured transmission loss of CW signals propagating from the MCP to sonobuoys with theoretical calculations of transmission loss (Fig. 2). As a result of calibration, corrections to the source level derived from the MCP accelerometers are determined (Table 4).

Previous efforts to calibrate the MCP [Fraser and Risley, 1991, Informal Report] did not

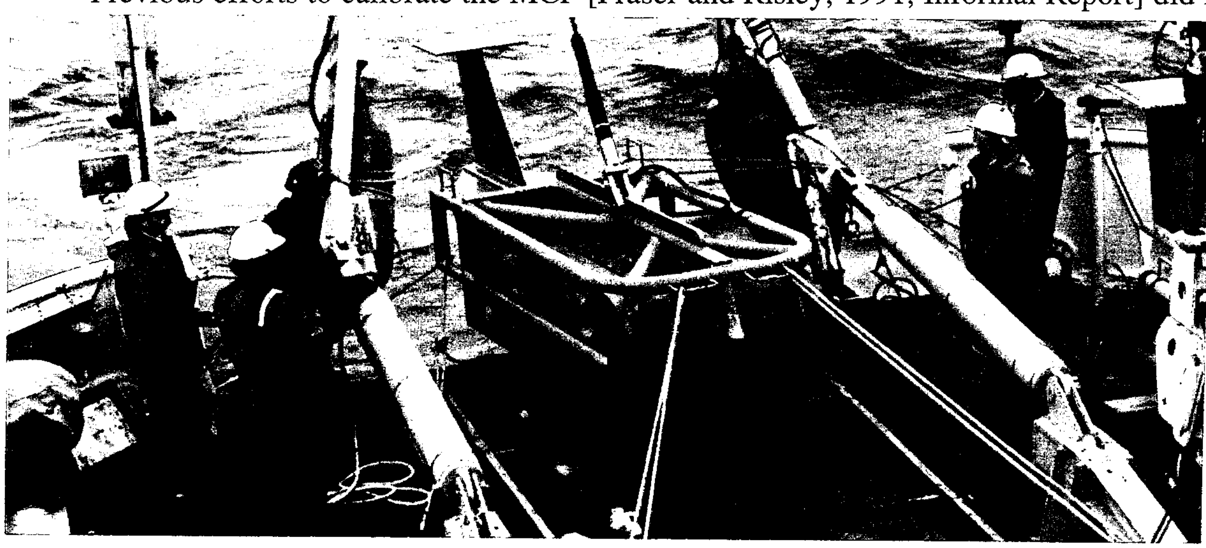

Figure 1: Photograph of the DREA Moving Coil Projector.

[1] The difference in pressure between the MCP interior and the surrounding water .

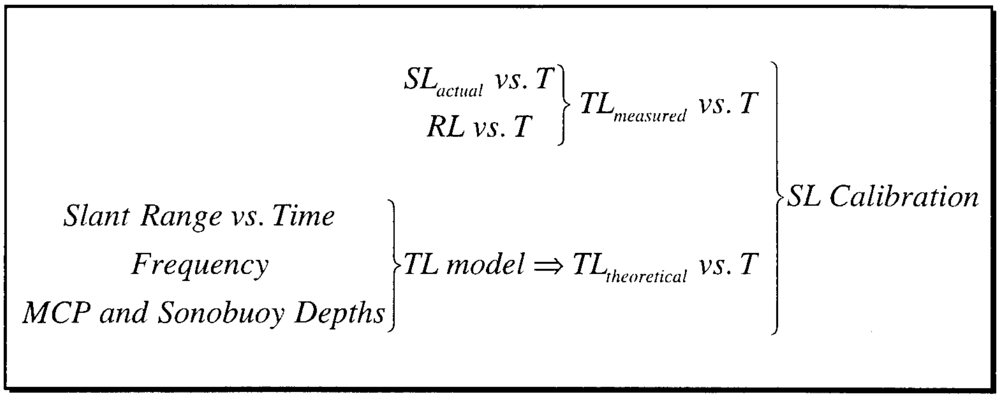

Figure 2: Schematic of the steps followed in calibrating the MCP. SL = MCP Source Level, RL = Sonobuoy Received Level, TL = Transmission Loss, T = Time.

consider the necessity to combine the signals from forward and aft accelerometers. They were also hampered by (a) MCP accelerometer signals with low signal-to-noise ratios and erratic behaviour and (b) the lack of direct measurements of the slant range from the MCP to the sonobuoys. Nonetheless, the suggestions of [Fraser and Risley, 1991, Informal Report] concerning experimental procedure and data reduction provided the foundation for this calibration exercise. This calibration also benefited from improvements in the signal-to-noise ratio of the MCP accelerometers following a substantial upgrade to the electronic circuitry of the monitoring system. Lastly, the winter sound speed profile allows a straightforward calculation of the theoretical transmission loss (Fig. 2), modeled simply by Lloyd's mirror interference.

2. Experimental Transmission Loss

Sea Trial

The calibration of the MCP was undertaken during *C.F.A.V. Quest* cruise Q211 on 3 December 1993 seaward of the edge of the Scotian Shelf near 42°59.4'N, 61°04.1'W. The experiment was conducted in approximately 1850 m of water. This water depth provides a horizontal range interval at the point of closest approach (CPA) for which bottom reflections are insignificant, thereby simplifying the calculation of a theoretical transmission loss for very low frequency (VLF) signals (Section 3).

The MCP was deployed at a nominal depth of 27.4 m (90 feet) and projected the suite of six VLF tones listed in Table 1. A seventh tone at 225 Hz was projected but not calibrated. The acoustic data were collected with the "short" array of an AN/SSQ 525A VLA Sonobuoy and an AN/SSQ 527B Omni Sonobuoy. In practice, one of the two VLA hydrophones failed so it also behaved as an omni-directional receiver. The sonobuoys were deployed with a depth setting of

Table 1: Nominal Source Level and frequency of tones projected by the MCP. The sensitivity of the accelerometers mounted on the forward and aft pistons and the sonobuoy hydrophones used to receive the signals are also tabulated.

Frequency (Hz)	Nominal Source Level (dB // 1 μPa @ 1m)	Sensitivity (dB // 1 V / 1 μPa @ 1 m)			
		Forward Accelerom.	Aft Accelerom.	VLA Sonobuoy	Omni Sonobuoy
4	150	-180.65	-179.89	-142.1	-146.6
7	150	-180.65	-179.89	-130.9	-140.4
12.5	150	-180.65	-179.89	-128.1	-135.5
22.5	150	-180.65	-179.89	-126.6	-130.5
41	150	-180.65	-179.89	-124.8	-127.1
72	150	-180.65	-179.89	-121.7	-123.8

304.8 m (1000 feet) on a previous pass of *C.F.A.V. Quest* across the nominal experimental location. To determine the slant range from the MCP to the sonobuoys, a barrel-stave projector mounted on the MCP was pinged (a burst of 15 cycles of a sinusoid every 10 seconds) at its resonance frequency of 800 Hz with a source level of 167 dB // 1 μPa @ 1m. From these slant ranges, the ship's speed past the sonobuoys was measured as 4.32 m/s (8.38 kts) during the calibration (Section 3).

Data Analysis

The signals from the forward and aft piston accelerometers, the monitor hydrophone mounted on the MCP, and the sonobuoys were digitized simultaneously at 2048 Hz and recorded on an 8 mm data cartridge by a Concurrent Corporation MC6400 data acquisition system. Following the cruise, the data were replayed and analyzed on a Digital Equipment Corporation AXP 3000 model 400 computer using software developed by DREA for acoustic data analysis [Farrell and Heard, 1992; Farrell, 1993].

Following Fraser and Risley [1991], a schematic of the playback and analysis sequence is shown in Figure 3.

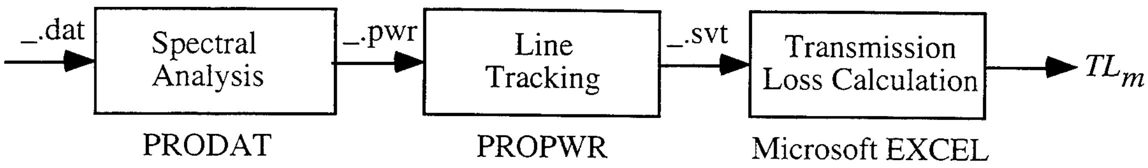

Figure 3: Analysis flowchart.

Relevant details about each of the steps in the analysis procedure are:

PRODAT: The time series data of the accelerometer and sonobuoy signals, in a DREA-standard *_.dat* file, are spectrum-analyzed using PRODAT [Farrell and Heard, 1992] to form a DREA-standard *_.pwr file.* The fast fourier transforms (FFTs) used 4096 points, with a 50% overlap between points used in successive FFTs. Three FFT's were averaged to obtain frames of power spectral density as a function of elapsed time. The centre separation between frames is 3 seconds which is sufficiently brief that nulls in the Lloyd's mirror interference pattern may be resolved (Section 3). Calibrations which account for different transducer sensitivities as a function of frequency are also applied in PRODAT.

PROPWR: A multiple line tracker, PROPWR, is applied to the *_.pwr* file to obtain time series of signal levels (with noise subtracted) for the accelerometer and sonobuoy signals simultaneously. A picket-fence correction is automatically applied to the signal peaks to improve the accuracy of the level estimates. For each frequency of interest, a frequency window for the signal and for upper and lower noise estimates is specified (Table 2). Output is to a signal vs. time, *_.svt*, file. These signal levels are not corrected for non-unity frequency bin widths in PRODAT, nor do they include

Table 2: Frequency windows for the signal and for upper and lower noise estimates which are applied when tracking narrowband lines and their signal level with PROPWR.

Nominal Frequency (Hz)	Signal Window (Hz)	Lower Noise Estimate (Hz)	Upper Noise Estimate (Hz)
4	3.75 - 4.25	3.20 - 3.70	4.30 - 4.80
7	6.75 - 7.25	6.20 - 6.70	7.30 - 7.80
12.5	12.25 - 12.75	11.70 - 12.20	12.80 - 13.30
22.5	22.25 - 22.75	21.70 - 22.20	22.80 - 23.30
41	40.75 - 41.25	40.20 - 40.70	41.30 - 41.80
72	71.75 - 72.25	71.20 - 71.70	72.30 - 72.80

the +1.7 dB correction for the Hanning window applied in PRODAT.

EXCEL: As the accelerometer signal can be converted to a calibrated source level[2] and the sonobuoy received levels can also be calibrated, the transmission loss is the difference of these two quantities at any point in time. This calculation, and display of the results, is readily achieved for the line tracked source and received levels in a spreadsheet such as EXCEL.

Combining Acceleration of the Forward and Aft Pistons to Obtain Source Level

Cotaras [1990] established that the acoustic power output, W, of a pair of piston projectors mounted back-to-back and operated in phase is a function of the volume displacement of the pistons,

$$W \propto (S_1 X_o)^2, \qquad (1)$$

in which S_1 is the surface area of one of the pistons and X_o is the peak displacement of the oscillating pistons. According to the accelerometer signals (Fig. 4), the forward and aft pistons have different displacements (X_f and X_a respectively) which requires that W_{actual} be written in terms of the displacement of both pistons,

$$W_{actual} \propto \left(S_1 \left(\frac{X_f + X_a}{2} \right) \right)^2. \qquad (2)$$

If the displacement of the aft piston is some fraction γ of the displacement of the forward piston, $X_a = \gamma X_f$, then W_{actual} may be written as

$$W_{actual} \propto \left(S_1 X_f \right)^2 \left(\frac{1+\gamma}{2} \right)^2. \qquad (3)$$

In terms of a source level, Equation 3 may be written as

$$SL_{actual} \propto 20\log\left(S_1 X_f \right) + 20\log\left(\frac{1+\gamma}{2} \right). \qquad (4)$$

Individually, the source levels indicated by the motion of the forward and aft pistons are

$$SL_f \propto 20\log\left(S_1 X_f \right) \qquad (5)$$

[2] Using a conversion from voltage to dB // 1 μPa @ 1m

$$SL_a \propto 20\log(S_1 X_f) + 20\log(\gamma). \qquad (6)$$

The difference between them is

$$\Delta SL = SL_a - SL_f = 20\log(\gamma). \qquad (7)$$

By taking the difference in source levels indicated by the motion of the forward and aft pistons, γ may be calculated as a function of time. This time-varying measurement of γ can then be substituted in Eq. 4, in effect correcting the source level as indicated by the front accelerometer only (SL_f) to obtain the actual source level, SL_{actual}:

$$SL_{actual} = SL_f + 20\log\left[\frac{1}{2}\left(1+10^{\Delta SL/20}\right)\right]. \qquad (8)$$

This procedure was implemented for all six MCP calibration frequencies; the 41 Hz result is illustrated in Fig. 4.

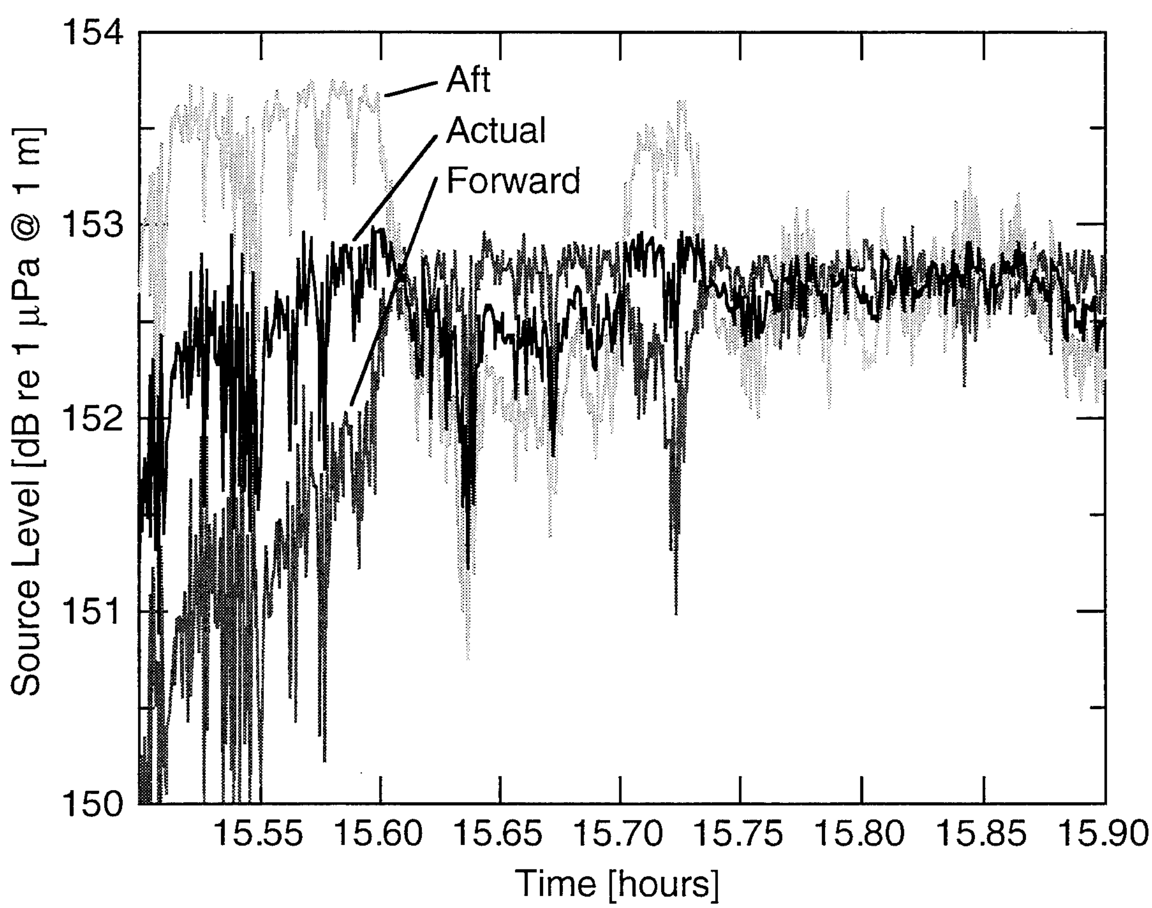

Figure 4: The 41 Hz source level of the DREA MCP (black line) as a function of time is determined by combining the source levels indicated by the accelerometers mounted on the forward (dark gray) and aft (light gray) pistons .

Two observations about the MCP source level (Fig. 4) should be emphasized. First, the forward and aft accelerometers do not have the same displacement at any particular time. Calibrations of MCP source level which have been made relative to the motion of one piston, and neglecting the other, are therefore suspect. Secondly, the source level of the MCP varies as a function of time. However, if the source levels of the accelerometers are recorded during an experiment, then the MCP may be used in quantitative derivations of acoustic properties such as transmission loss by combining the source levels in the previously-described manner.

Inter-Piston Phase Differences and Projector Directionality

The previous analysis assumed that the signals from both MCP pistons arrive at the receiver in phase. In fact, if the signals exhibit a phase difference ϕ the source level (SL) will be reduced by $-10\log[(1+\cos\phi)/2]$ decibels from the in-phase level. In order to keep this effect below 1 dB, the phase difference must not exceed 54°. Two independent conditions that could introduce such a phase difference are (a) an intrinsic phase lag δ between the piston displacements and (b) a direction-dependent phase difference caused by the inter-piston distance d, i.e. $\phi_d = kd\cos\theta$, in which θ is the angle between the fore-aft direction and the receiver direction. The maximum direction-dependent phase difference in radians is therefore kd. For a piston separation of 2.4 m and a sound speed of 1505 m/s, the kd values for the seven MCP frequencies are shown in Table 3, expressed both in radians and degrees. If the phase-related SL variations are to be kept below 1 dB, any intrinsic phase difference between the pistons must be less than $\delta_+ = 54° - kd$ degrees, also shown in Table 3. From the piston accelerometer time series data (Appendix A), the minimum, median, and maximum intrinsic phase difference have been determined at all frequencies during the time span of the calibration run; they are shown in Table 3.

Table 3: Theoretical maximum and measured phase differences between the fore and aft MCP pistons at all projected frequencies.

f [Hz]	4	7	12.5	22.5	41	72	225
kd [rad]	0.04	0.07	0.13	0.23	0.41	0.72	2.25
kd [deg]	2	4	7	13	14	41	129
δ_+ [deg]	**52**	**50**	**47**	**41**	**30**	**13**	**–**
δ_{min} [deg]	13	1	1	0	0	13	53
δ_{median} [deg]	**24**	**22**	**9**	**2**	**3**	**20**	**63**
δ_{max} [deg]	34	47	24	14	16	26	114

The range of measured phase values at 4–41 Hz is within acceptable bounds; the phase at 72 Hz is marginal. At 225 Hz the *kd* value is already too high; the MCP is a directional source at this frequency and could not be expected to be omnidirectional above about 90 Hz. For this reason the 225 Hz tone was dropped from the calibration exercise.

Received Level on Sonobuoy

Two sonobuoys, the "short array" of an AN/SSQ 525A VLA and an AN/SSQ 527B Omni, were used as receivers in this calibration exercise. There is evidence that only one of the two hydrophones in the VLA "short array" was operating. The VLA hydrophones are spaced 1.83 m (6 feet) apart, therefore arrivals at frequencies less than approximately 410 Hz will be in phase regardless of arrival angle. However when ambient noise spectra at low frequencies are compared (Fig. 5), the VLA received levels are approximately 6 dB too low, as would be

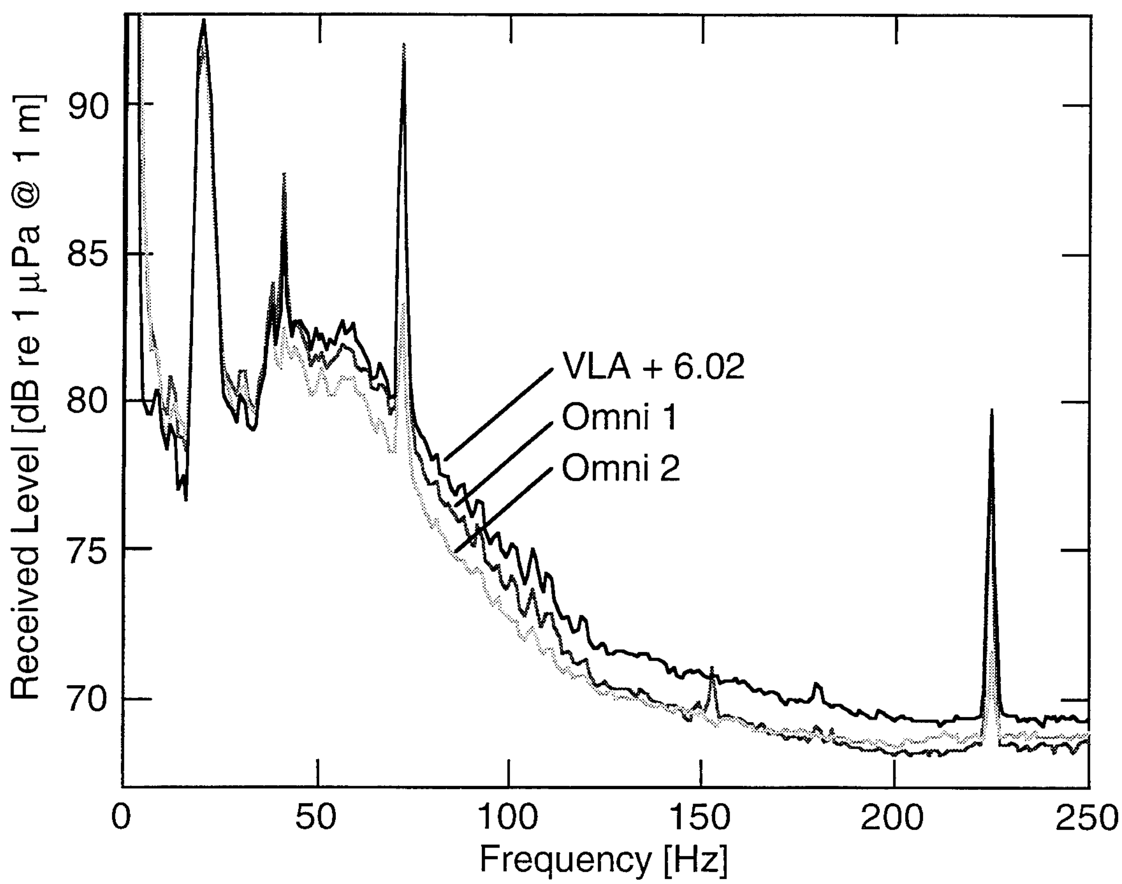

Figure 5: Received level on three sonobuoys deployed during the calibration of the MCP. Each frequency bin represents a median average across 324 spectra (40.5 minutes). The Omni 1 and VLA buoys are used in the calibration. Ambient noise measurements with Omni 2 are used in correcting for differences in sensitivity between the VLA and Omni sonobuoys.

expected if only half the acoustic power were present.

A second indication that one hydrophone is unserviceable is the lack of nulls at higher frequencies at which the short array becomes directional. As the received levels are a convolution of the array beampattern with the directionality of the ambient noise, there should be a decrease in received level at frequencies where the wavelength of vertical arrivals gives rise to destructive interference. This should occur at approximately 410 Hz and its harmonics, but is not present in the spectra from the VLA buoy (not shown). On the basis of these observations, the received levels of the VLA buoy have been increased by 6.02 dB (Fig. 5).

The offset between the received levels of the sonobuoys in response to ambient noise[3] is a measure of the differences in sensitivity of the sonobuoys. Fig. 5 includes the spectra from a third sonobuoy, Omni 2 - an AN/SSQ 527B, deployed during an earlier experiment in the same area and still broadcasting. As the spectra from the two Omni sonobuoys coincide at higher frequencies, the average of their received levels is treated as an absolute measurement of the ambient noise. The sensitivity of the Omni 1 and VLA buoys adjusted to this reference level in the immediate vicinity of the MCP projector frequencies (Table 1) requires corrections of -0.05, -0.4, -0.7, and 0.1 dB for the Omni buoy and -0.4, -0.4, -1.3, and -1 dB for the VLA buoy at the 22.5, 41, 72 and 225 Hz MCP projector frequencies respectively. No sensitivity corrections are applied below 20 Hz where the noise on these types of sonobuoys is dominated by self noise.

Transmission Loss

The transmission loss as a function of time at a given frequency is the difference between the source level of the MCP and the time coincident measurements of received level on the sonobuoys (Fig. 2). The transmission loss for the Omni and VLA sonobuoys at 41 Hz is presented in Fig. 6.

3. Theoretical Transmission Loss

If the projector source level as indicated by the piston accelerometers is correct, then the experimental transmission loss should match the modeled transmission loss, assuming again that the model is accurate. In this section we invoke a simple transmission loss model based on the Lloyd's mirror effect and validate it against a more complex model that takes into account the actual sound speed profile and bottom reflection.

[3] At frequencies not projected by the MCP (Table 1).

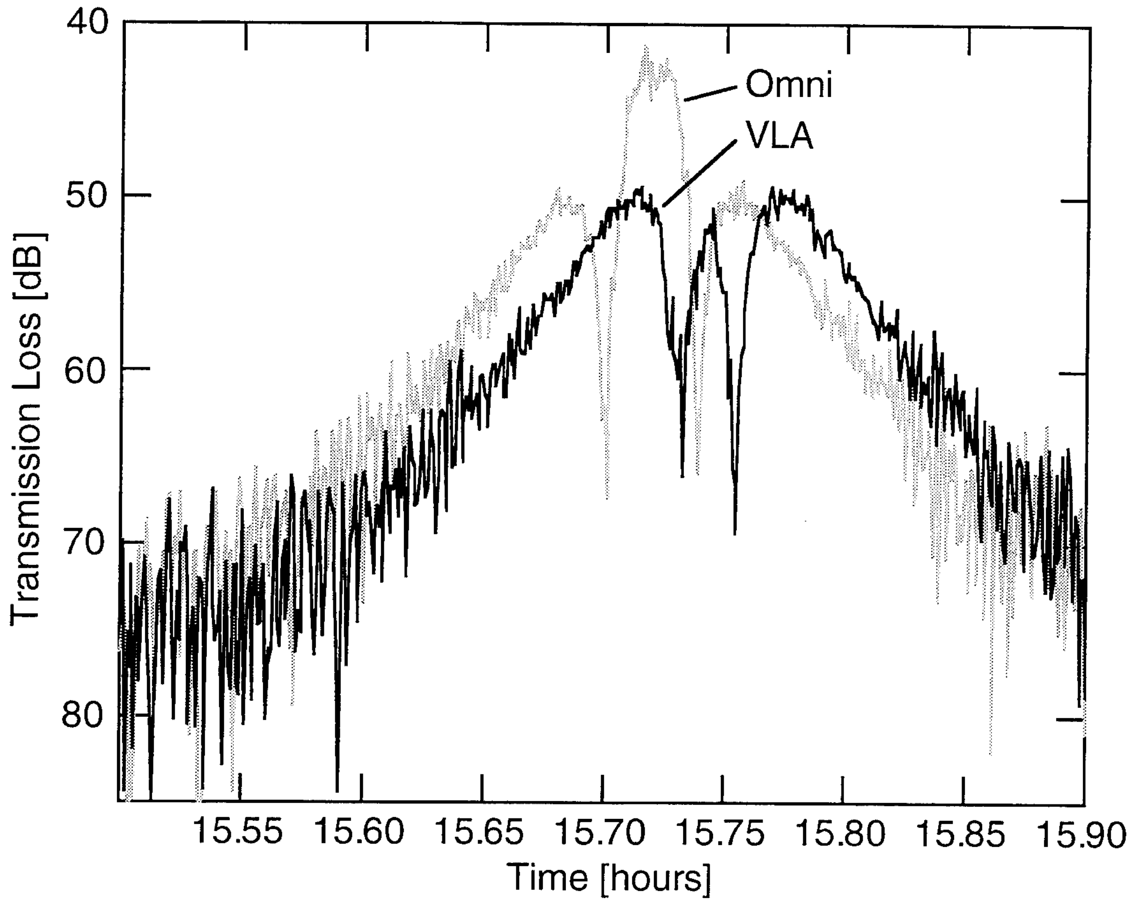

Figure 6: Transmission Loss at 41 Hz as a function of time for the two sonobuoys used as receivers in the calibration of the MCP. Note the different CPA times (time offset) and slant-range minimums (transmission loss minimum).

Geometry

Referring to Fig. 7, and assuming straight-line ray paths, the slant range L_1 between the source at depth d_1 and the receiver at depth d_2 at horizontal range r is

$$L_1 = \sqrt{r^2 + (d_2 - d_1)^2}\,. \qquad (9)$$

In addition to this direct path, there is a surface-reflected path which is equivalent to a straight-line path to an image source at depth $-d_1$, the slant range in this case being

$$L_2 = \sqrt{r^2 + (d_2 + d_1)^2} = \sqrt{L_1^2 + 4d_1 d_2}\,. \qquad (10)$$

The source often does not move exactly on a radial path towards and away from the receiver; in the simplest case, the source describes a closest-point-of-approach (CPA) path at constant speed v as in Fig. 7. The horizontal range r is then given by

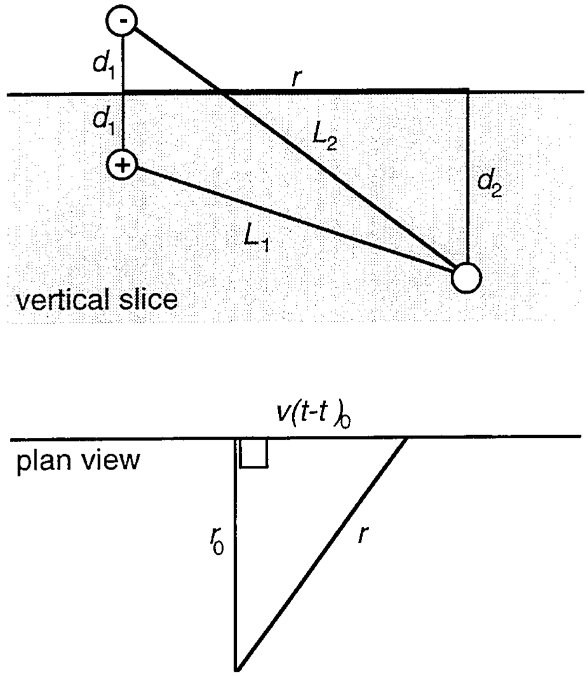

Figure 7: Geometry of the source and receiver in the calibration of the MCP.

$$r = \sqrt{r_0^2 + v^2(t - t_0)^2}\,, \qquad (11)$$

in which r_0 is the CPA range and t_0 is the time of CPA. The CPA slant range is then

$$L_{10} = \sqrt{r_0^2 + (d_2 - d_1)^2}\,, \qquad (12)$$

so the slant range L_1 can be rewritten directly as a function of time t and the three parameters L_{10}, v, and t_0:

$$L_1 = \sqrt{L_{10}^2 + v^2(t - t_0)^2}\,. \qquad (13)$$

In our calibration field trial, we measured the slant range L_1 directly using a 800 Hz ping generated on a barrel-stave transducer mounted on the MCP body. The time-of-flight of the pings between the MCP and the receiver multiplied by the speed of sound (1505 m/s) provides L_1 at a sequence of clock times. A simple three-parameter curve can be fit to these values, as illustrated in Fig. 8 for the two sonobuoys; the curve fit parameters are displayed in Table 4.

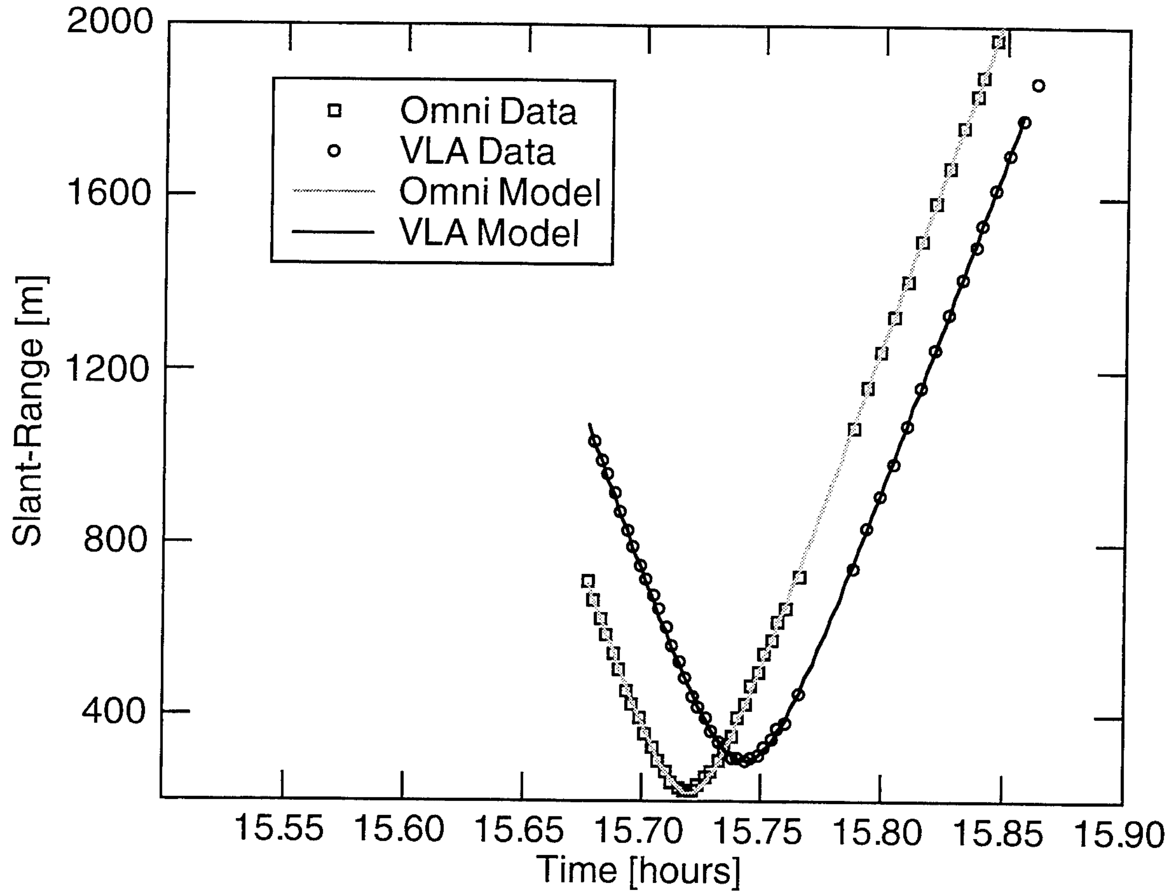

Figure 8: Slant range from the MCP to the receiving sonobuoys.

Table 4: Parameters of projector CPA on two sonobuoys.

Sonobuoy	Omni	VLA
v [m/s]	4.32	4.32
L_{10} [m]	219	292
t_0 [h]	15.7198	15.7433

Lloyd's Mirror Transmission Loss Calculations

Referring back to Fig. 7, we can model the acoustic field at the receiver as the interference between the source and its out-of-phase image, both considered as omnidirectional sources. Introducing the wavenumber $k = 2\pi f / c$, where f is the source frequency and c is the speed of sound, the received pressure is

$$P = P_0 R_0 \left[\frac{e^{ikL_1}}{L_1} - \frac{e^{ikL_2}}{L_2} \right], \qquad (14)$$

in which P_0 is the pressure at reference distance R_0 (usually 1 metre) from the point source considered in isolation. The transmission loss in decibels is then

$$TL = 10\log|P_0/P|^2 = 10\log\left[\frac{1}{L_1^2} + \frac{1}{L_2^2} - \frac{2}{L_1 L_2}\cos[k(L_1 - L_2)] \right], \qquad (15)$$

in which R_0 has been assumed to be 1 m and all distances are measured in metres.

To model TL as a function of time during the CPA pass, we first re-generate L_1 from Eq. (13) using the parameters from Table 4 and then calculate L_2 from the second part of Eq. (10) using an assumed value of the product $d_1 d_2$. L_1 and L_2 are then combined with the acoustic wavenumber k to calculate TL using Eq. (15). Note that the acoustic frequency only enters the calculation through the interference term, giving rise to deep nulls in the interference pattern whose positions vary with frequency. The parameter $d_1 d_2$ must be adjusted so that the interference nulls in the modeled TL match those in the measured TL for all frequencies that exhibit dips in received level. This can be done easily in a computer spreadsheet containing both experimental and modeled TL values plotted together as a function of time.

Validation of the Lloyd's Mirror Transmission Loss Model

The Lloyd's mirror (LM) transmission loss model assumes an isospeed ocean (i.e. no refraction of acoustic rays), with no bottom-reflected paths. If LM proves to be an adequate portrayal of the acoustic field during the calibration run, then the reduction of the calibration data is greatly simplified; but first, we must validate the LM against a more complex model that includes refraction and bottom reflection effects. For this validation, we chose to use the SAFARI fast-field code [Schmidt, 1988], which is capable of computing a wave-theory transmission loss in a layered environment including an ocean with a depth-dependent sound speed and a realistic seabed. Refraction effects, surface interference effects, and bottom-reflected paths are all taken into account automatically with SAFARI.

The sound speed profile measured during the calibration run using an expendable sound velocimeter (XSV) is shown in Fig. 9. The XSV provides many more data points than SAFARI can handle and also introduces some scatter, so we generated a simplified profile for SAFARI modeling, also illustrated in Fig. 9. The depths of the MCP and omni sonobuoy receiver are also indicated. One can see that the MCP is in an upward-refracting surface duct but the receiver is

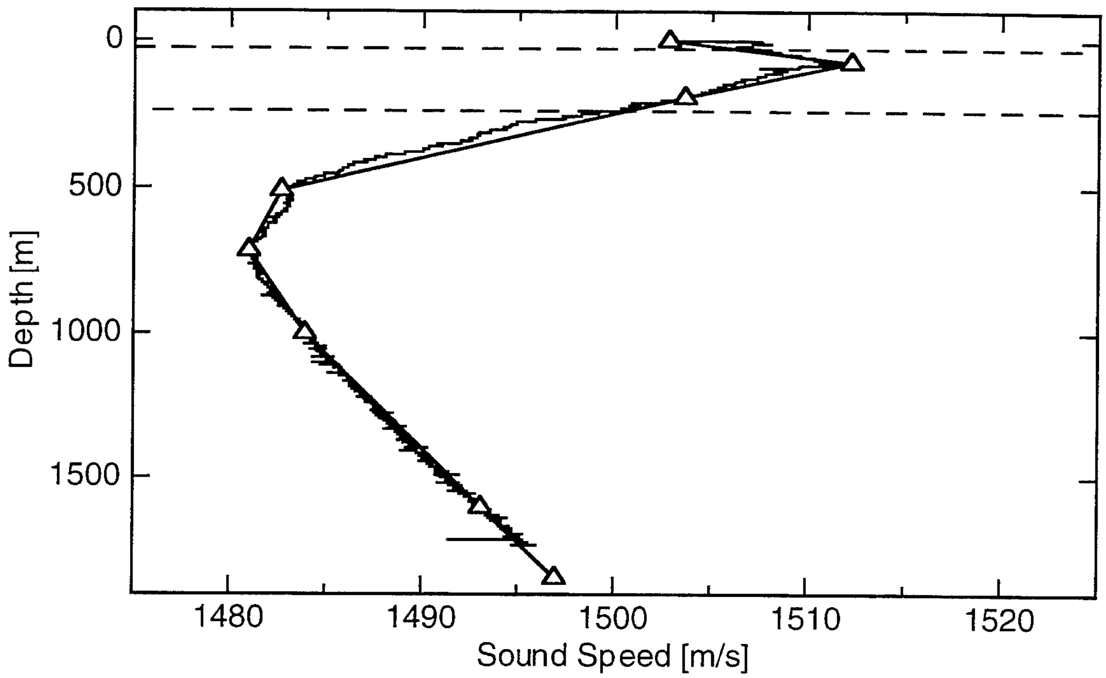

Figure 9: The sound speed profile at the calibration site: solid lragged ine–as measured by an expendable sound velocimeter; open triangles–as simplified for the SAFARI model; dashed lines–depths of source (shallow) and omni sonobuoy receiver (deep).

below the surface duct in a downward-refracting environment. We chose a value of 1505 m/s to represent the "average" sound speed for LM and other calculations that assume an isospeed environment.

To compare the predictions of SAFARI and LM in this environment, we assumed a source depth of 28.6 m and a receiver depth of 246.7 m, values representative of the calibration experiment. We introduced a single-layer seabed at depth 1845.6 m having a compressional sound speed of 1550 m/s and a specific gravity of 1.6; other seabed parameters of lesser importance were: shear speed 100 m/s, compressional attenuation .5 dB/wavelength, and shear attenuation 2 dB/wavelength. This bottom model is thought to be representative of the soft sediments at the site. The SAFARI transform size was chosen to be 4096 points, and phase speed limits were chosen at each frequency by examining the SAFARI integrand to ensure that all significant energy was accounted for (especially the steep ray paths) and that the resulting field was computed with sufficient range resolution to display the interference nulls.

The comparison of TL vs. range computed with SAFARI and LM is shown in Fig. 10 for the 41 Hz case and in Appendix B for all frequencies: 4, 7, 12.5, 22.5, 41, and 72 Hz. In all cases LM reproduces the SAFARI results out to about 1 km range, after which bottom-reflection effects begin to have significant effect in the SAFARI model. In particular, the agreement

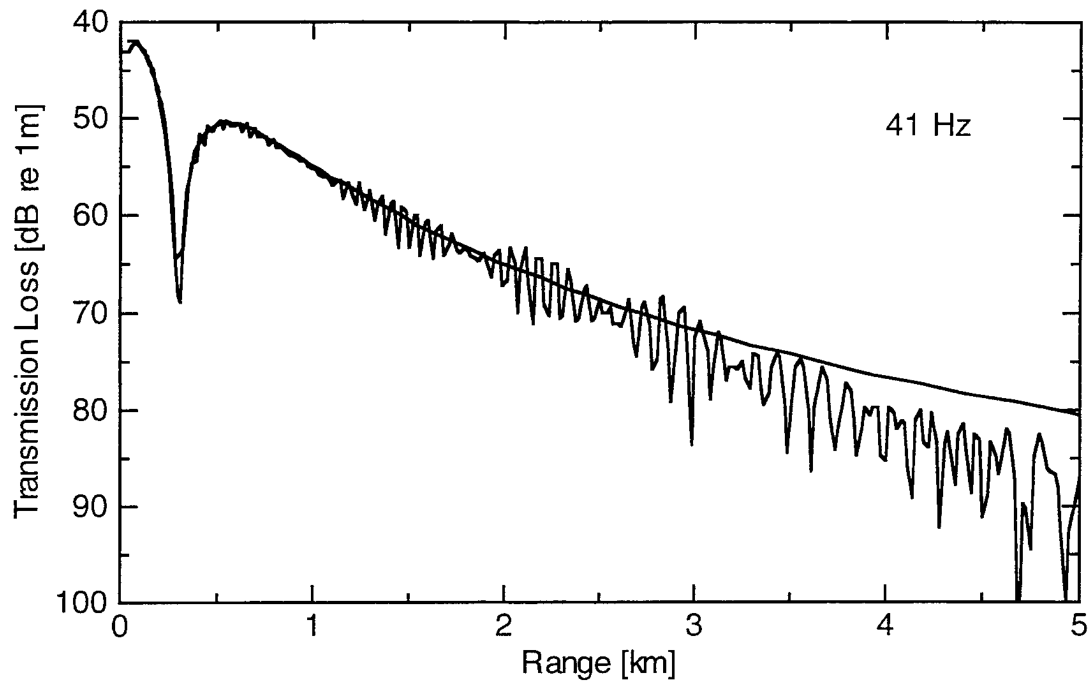

Figure 10: TL vs. range according to SAFARI (ragged line) and Lloyd's mirror (smooth line), between a 41 Hz source at 28.6 m depth and a receiver at 246.7 m depth.

between the models is perfect with respect to the location of the interference nulls at 41 and 72 Hz . At a ship speed of 4.32 m/s, the LM model should be adequate for calculating transmission loss within 4 minutes of CPA, spanning the TL data we will present in the next section.

4. Results

The culmination of the exercise to calibrate the MCP is a comparison of experimental transmission loss (section 2) with theoretical transmission loss (section 3). This comparison is illustrated for the Omni and VLA sonobuoys in Figures 11 and 12 respectively; measurements of the experimental transmission loss are marked by dots while the theoretical transmission loss is marked by the continuous gray line. The scatter in the experimental transmission loss is greatest at 4 Hz, particularly for the Omni buoy (Fig. 11a), because of the poor signal-to-noise ratio.

There is general agreement between experimental and theoretical transmission loss; the position of the Lloyd's mirror nulls are matched and so are the transmission loss levels, particularly for the peaks in the Lloyd's mirror interference. There is reasonable agreement for the nulls, though they are not as pronounced in the experimental transmission loss because there is some temporal averaging of the received signals which was required to produce reliable estimates of the power spectral density (section 2).

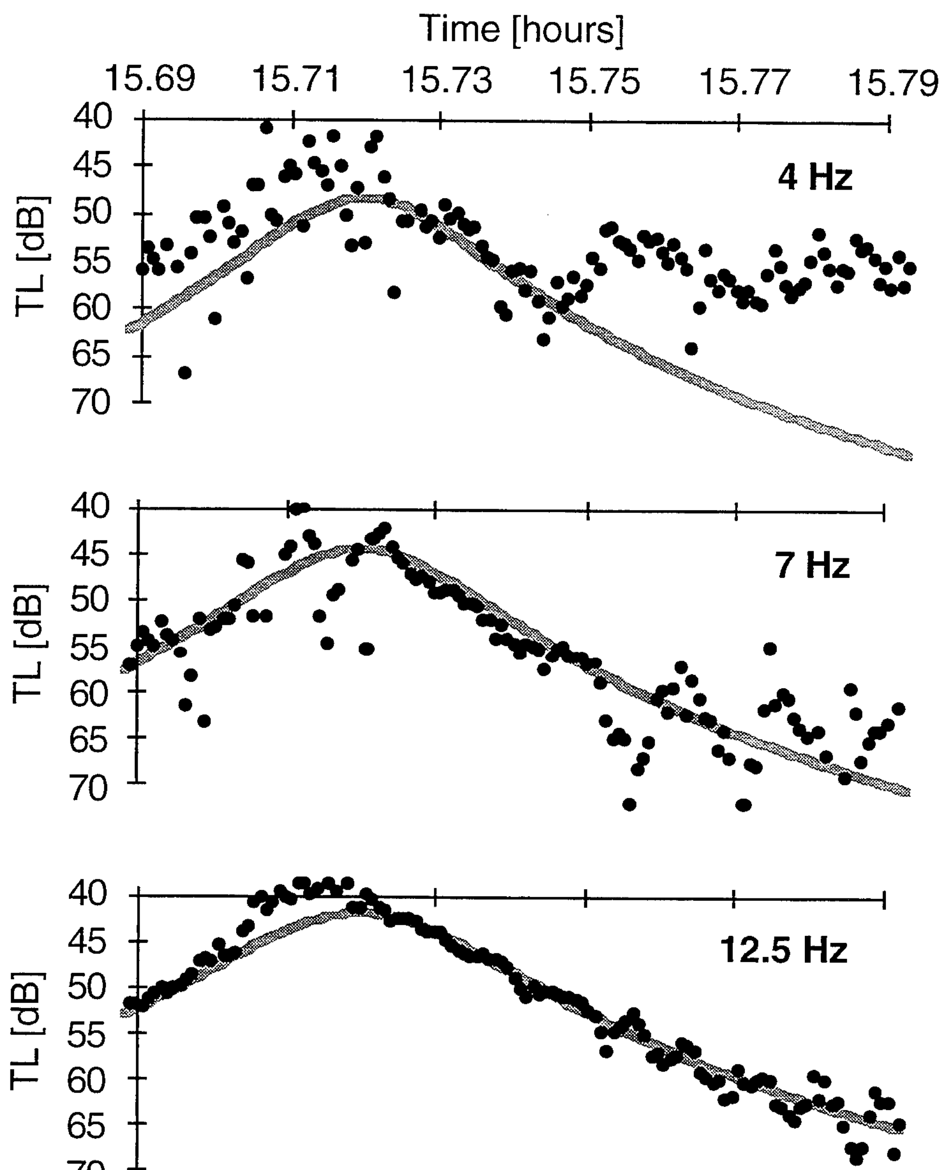

Figure 11a: *Experimental Transmission Loss measurements on the Omni buoy (dots) are overlain by the theoretical Transmission Loss (gray line) at 4, 7, and 12.5 Hz.*

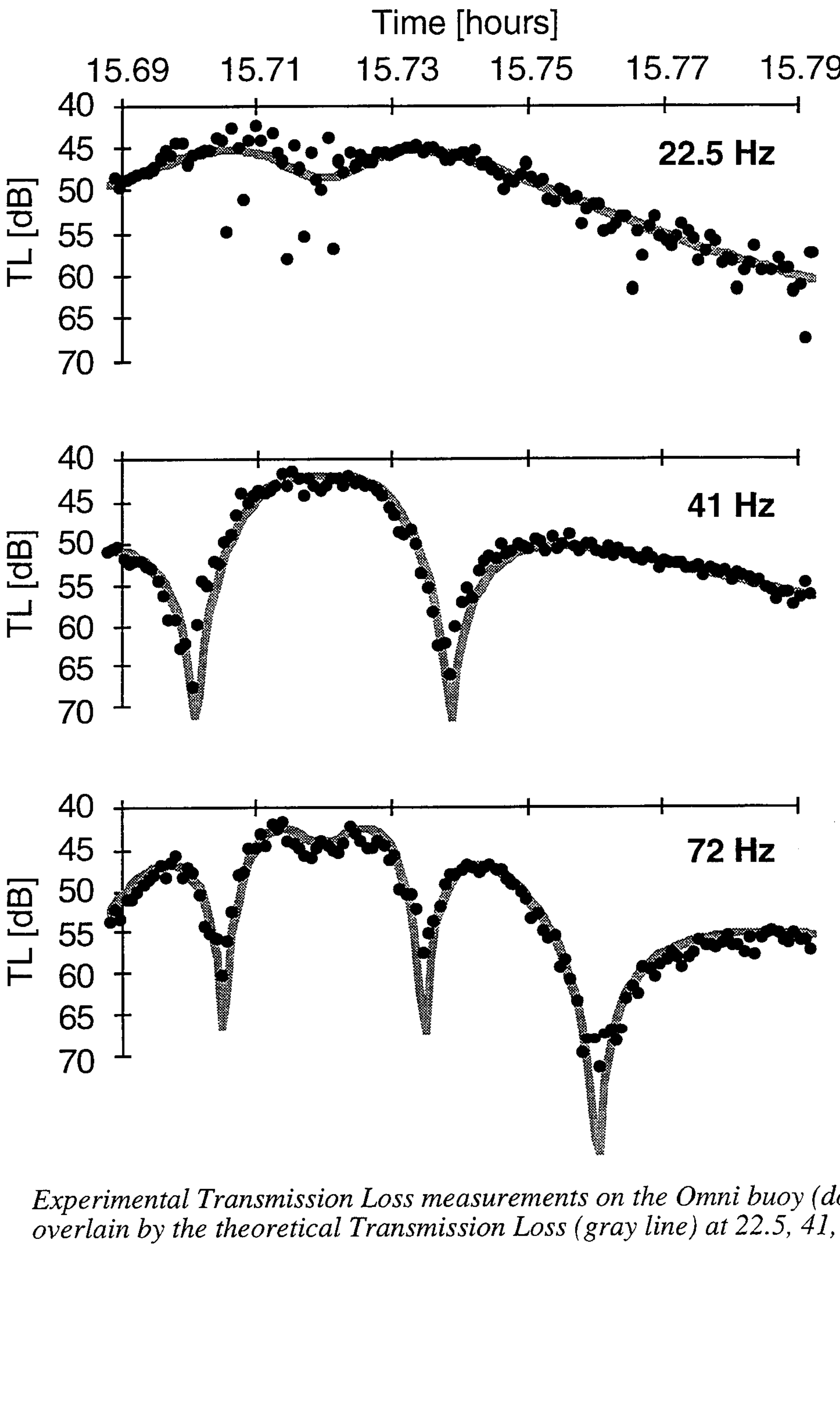

Figure 11b: *Experimental Transmission Loss measurements on the Omni buoy (dots) are overlain by the theoretical Transmission Loss (gray line) at 22.5, 41, and 72 Hz.*

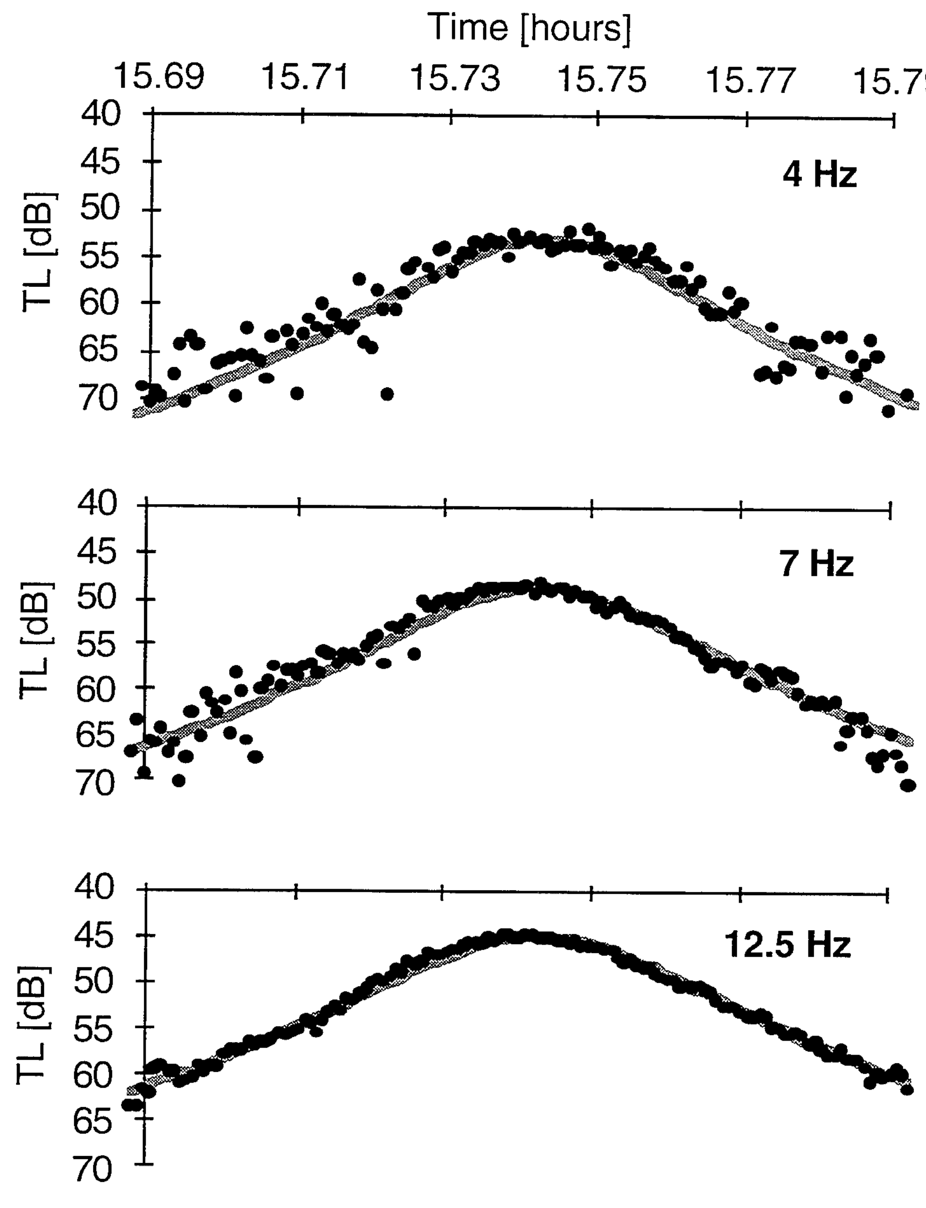

Figure 12a: *Experimental Transmission Loss measurements on the VLA buoy (dots) are overlain by the theoretical Transmission Loss (gray line) at 4, 7, and 12.5 Hz.*

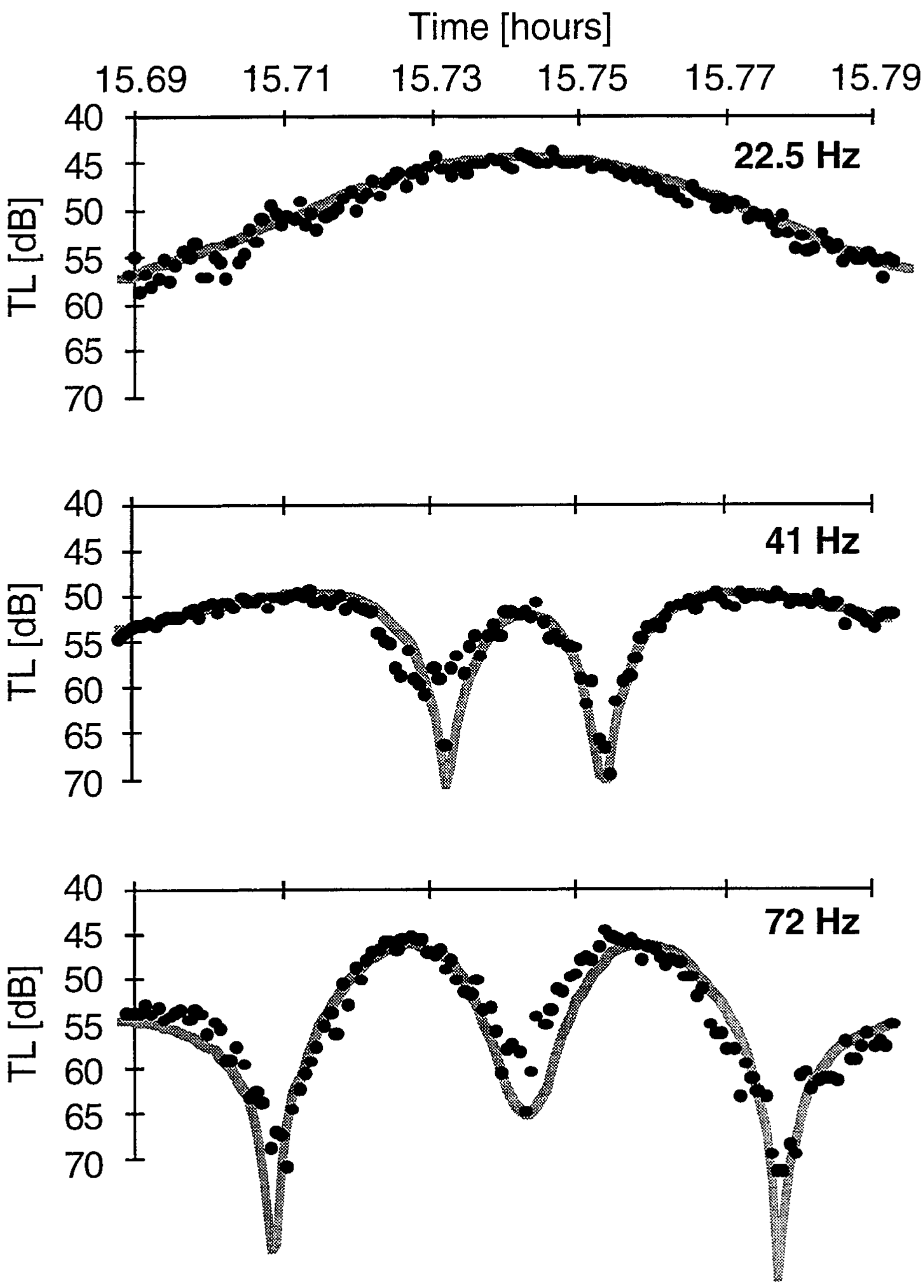

Figure 12b: *Experimental Transmission Loss measurements on the VLA buoy (dots) are overlain by the theoretical Transmission Loss (gray line) at 22.5, 41, and 72 Hz..*

The experimental transmission loss measurements include corrections to the source levels derived from the forward and aft accelerometer signals (Eq. 8) to qualitatively improve the fit of the experimental to the theoretical measurements. These corrections to MCP source level are listed in Table 5. They are limited to the higher frequencies of 41 and 72 Hz where +1 dB and +2.5 dB have been added to the source levels.

The choice of a source level correction at any frequency considered the simultaneous fit of the experimental and theoretical transmission loss on both sonobuoys. Considering a sonobuoy in isolation, one might be inclined to introduce source level corrections which would improve its fit to the theoretical transmission loss. As an example, consider the experimental transmission loss values on the Omni buoy at 7 Hz which are somewhat too large post-CPA and those at 12.5 Hz which are too low pre-CPA. The simultaneous measurements on the VLA sonobuoy show no requirement for any source level corrections as the experimental and theoretical values coincide. Another example is the experimental transmission loss at 72 Hz on the VLA sonobuoy past-CPA which appears phase shifted relative to the theoretical values. It is not an incorrect CPA time as this is determined from the slant ranges, and the Lloyd's mirror peaks and nulls match the experimental transmission loss at the other frequencies. Nor does it appear to be unaccounted source level fluctuations as a similar feature is not observed on the Omni sonobuoy. In this case, it is likely that the source level fluctuations are due to some directionality of the MCP because of the position of the VLA sonobuoy relative to the source (section 2, Table 3).

Table 5: Corrections to the source level of the MCP as determined from combining signals from accelerometers mounted on the forward and aft pistons.

Frequency (Hz)	Correction (dB)
4	0
7	0
12.5	0
22.5	0
41	+1
72	+2.5

5. Conclusions and Recommendations

1) The MCP source level varies as a function of time in accordance with the operating state of the projector. Actual source levels may be determined instantaneously by combining signals from accelerometers mounted on the forward and aft pistons in an appropriate manner (Eq. 8). This methodology was validated through a comparison of experimental and theoretical transmission loss on two sonobuoys. In order to use the source level of the MCP in any quantitative analysis, it is imperative that signals from the accelerometers mounted on the forward and aft pistons have good signal-to-noise ratios and that these signals be recorded continually.

2) No corrections are required to the source level of the MCP as derived from the accelerometer signals for frequencies less than 30 Hz. In this calibration exercise, corrections to the MCP source level were only required at 41 and 72 Hz.

3) At frequencies greater than approximately 90 Hz, the MCP becomes a directional source and should not be used in experiments which require an omnidirectional acoustic source. As frequency increases, so will the source level variations due to the direction-dependent phase difference which arises from the separation of the forward and aft pistons. This effect is compounded by the phase difference between the forward and aft pistons which becomes unacceptably large.

4) A control system capable of maintaining a constant source level for up to eight tonals generated by the MCP is desirable for future MCP operations. This system would continually monitor the accelerometers to determine instantaneous source level (in the manner prescribed in this document) and then make appropriate adjustments to the drive signal for each tonal.

5) Fluctuations in the source level of the MCP may be minimized by keeping the operating state of the MCP as steady as possible, for example, by avoiding variations in ship speed and course in so far as possible. Further, the nose down pitch (-20°) of the MCP under tow introduces an offset in differential pressure of approximately 1 psi between the pistons, which translates into approximately one third of the allowable piston displacement. To ensure that pistons remain in the linear portion of the coil and away from the stops, the offset in differential pressure should be accommodated by displacing both pistons from their equilibrium positions.

References

Cotaras, F. D., 1990, The source level of piston projectors, DREA Note SA/90/3, 8 pp.

Farrell, J. B., 1993, PROPWR: A versatile tool for 1/3 octave processing and narrowband line tracking, DREA Technical Communication 93/303, 44 pp.

Farrell, J. B., and G. J. Heard, 1992, PRODAT: A versatile tool for spectral analysis and display, DREA Technical Communication 92/309, 72 pp.

Fraser, I. A., and W. C. Risley, 1991, An at-sea calibration of DREA's low-frequency moving-coil projector, DREA Note UA/91/7, 18 pp.

Schmidt, H., 1988, SAFARI: Seismo-Acoustic Fast field Algorithm for Range-Independent environments, User's Guide, SACLANT Undersea Research Centre Report SR-11, 152 pp.

Appendix A: Source Level and Inter-Piston Phase

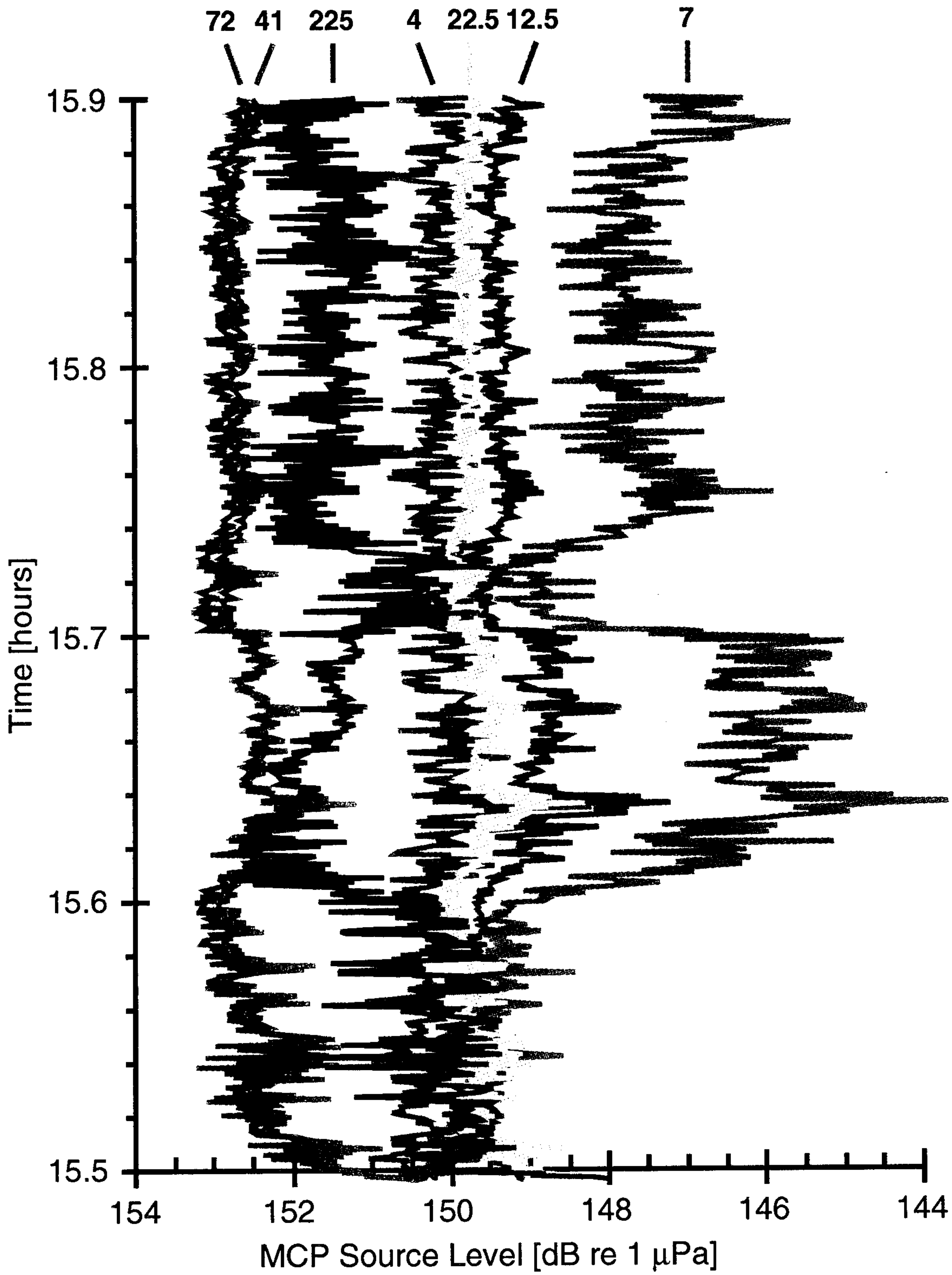

Figure A1: *Source level of the DREA MCP at 4, 7, 12.5, 22.5, 41, 72, and 225 Hz derived from accelerometers mounted on the forward and aft pistons.*

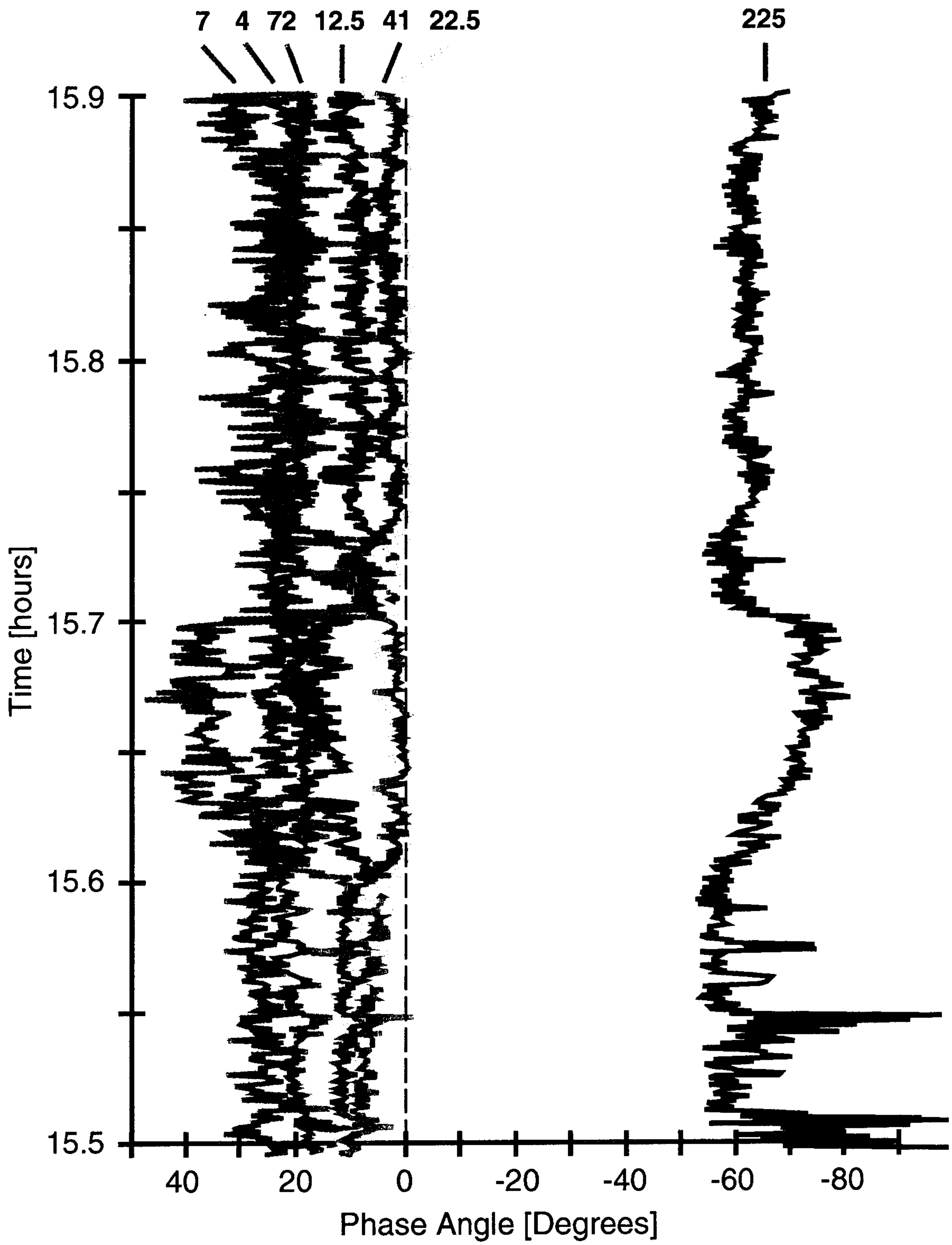

Figure A2: *Phase angle between the accelerometers mounted on the forward and aft pistons of the DREA MCP at 4, 7, 12.5, 22.5, 41, 72, and 225 Hz.*

Appendix B: Comparison of TL Calculated using SAFARI and LM

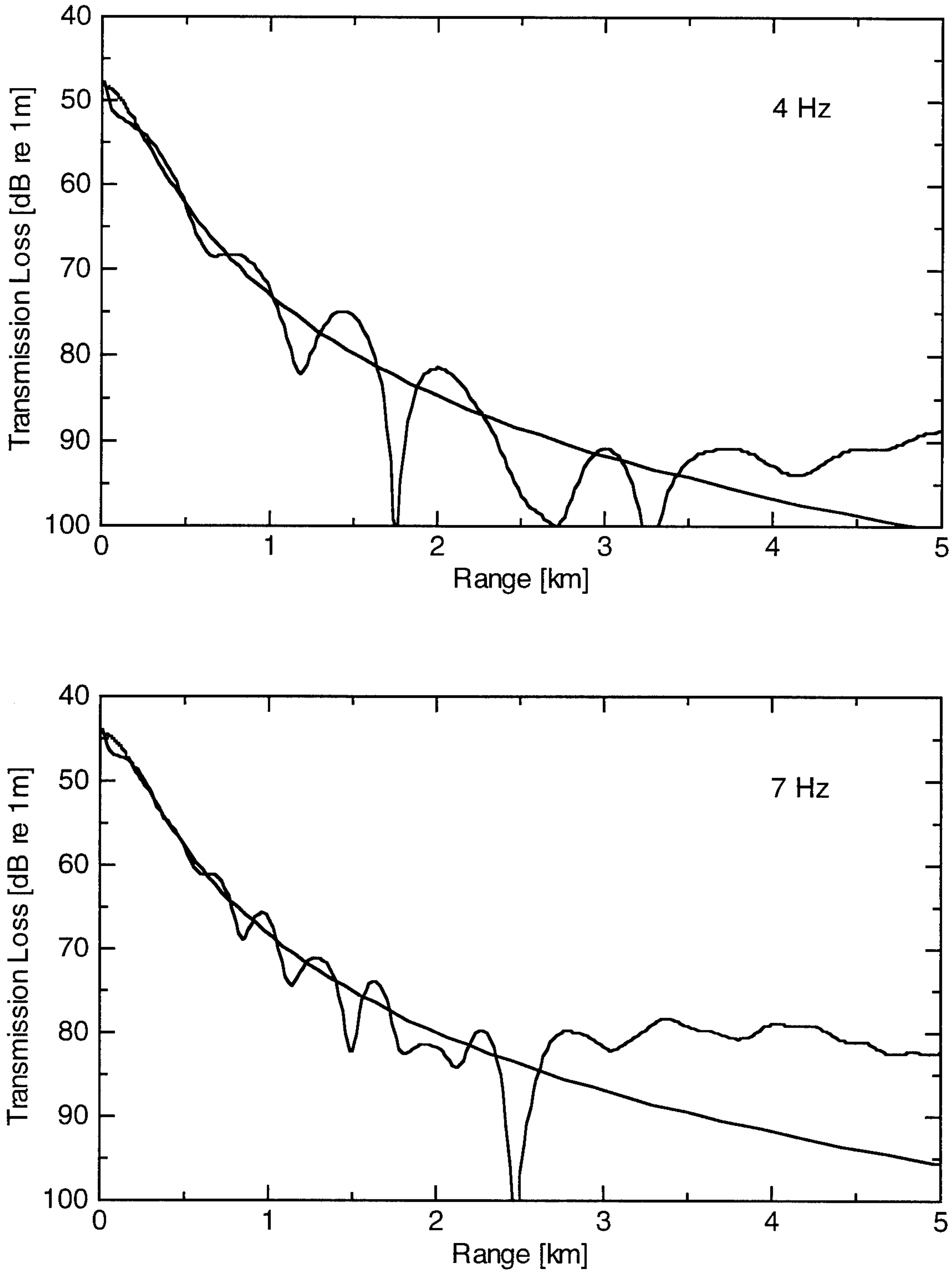

Figure B1: *TL vs. range according to SAFARI (ragged line) and Lloyd's mirror (smooth line), between a source at 28.6 m depth and a receiver at 246.7 m depth: 4 and 7 Hz.*

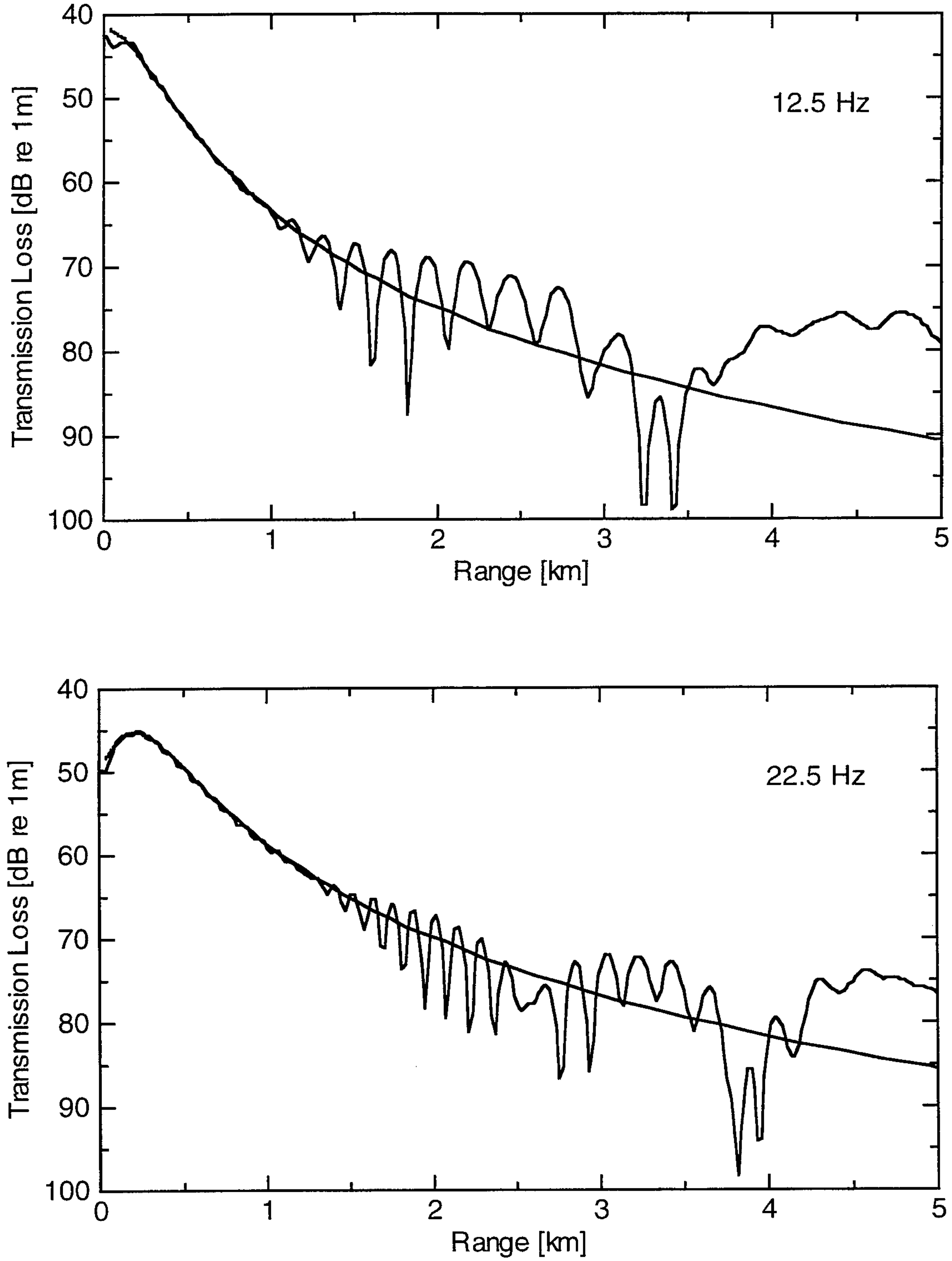

Figure B2: *TL vs. range according to SAFARI (ragged line) and Lloyd's mirror (smooth line), between a source at 28.6 m depth and a receiver at 246.7 m depth: 12.5 Hz and 22.5 Hz.*

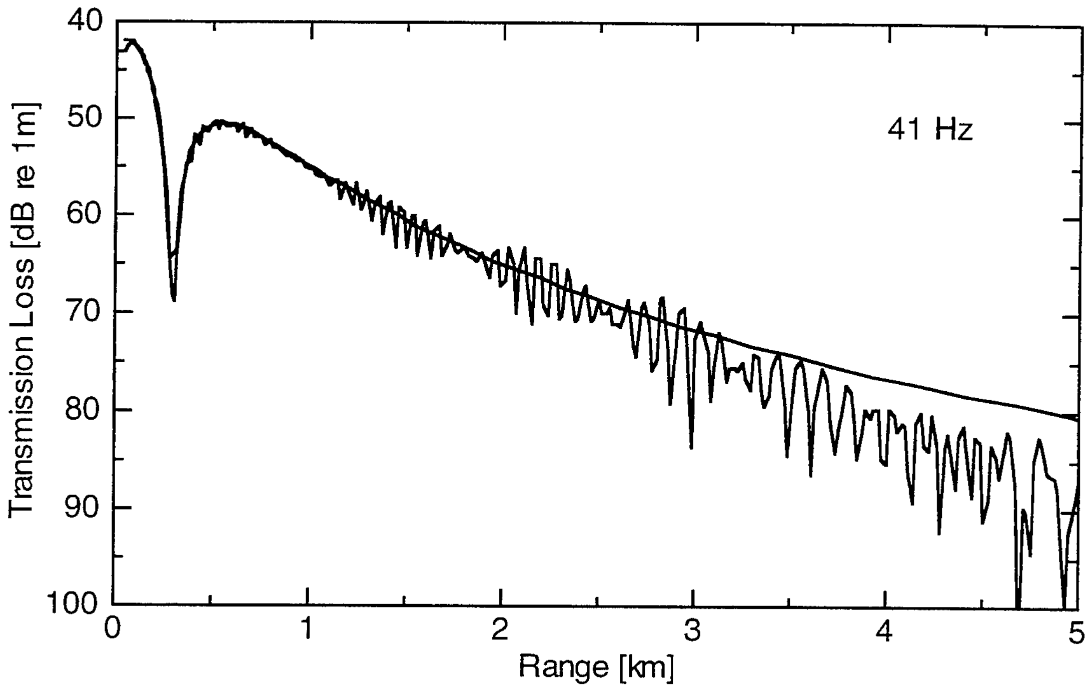

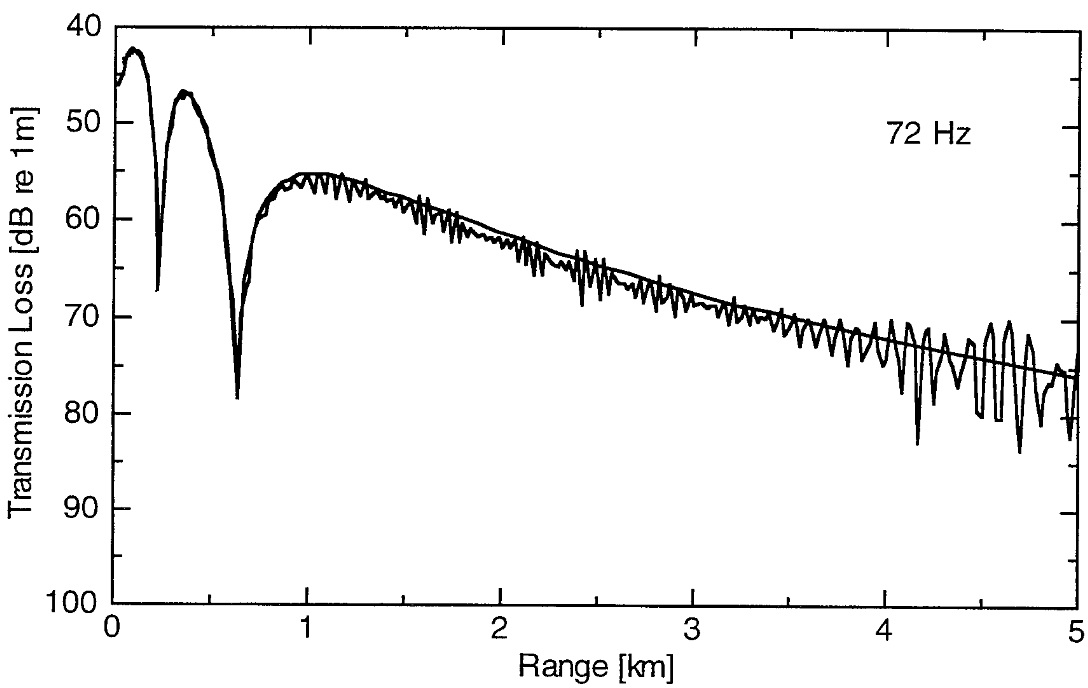

Figure B3: *TL vs. range according to SAFARI (ragged line) and Lloyd's mirror (smooth line), between a source at 28.6 m depth and a receiver at 246.7 m depth: 41 and 72 Hz.*

DOCUMENT CONTROL DATA

(Security classification of title, body of abstract and indexing annotation must be entered when the overall document is classified)

1. ORIGINATOR (The name and address of the organization preparing the document. Organizations for whom the document was prepared, e.g. Establishment sponsoring a contractor's report, or tasking agency, are entered in section 8.)

Defence Research Establishment Atlantic
P.O. Box 1012, Dartmouth, N.S. B2Y 3Z7

2. SECURITY CLASSIFICATION (Overall security of the document including special warning terms if applicable.)

Unclassified

3. TITLE (The complete document title as indicated on the title page. Its classification should be indicated by the appropriate abbreviation (S,C,R or U) in parentheses after the title.)

Source Level Calibration of the DREA Moving Coil Projector

4. AUTHORS (Last name, first name, middle initial. If military, show rank, e.g. Doe, Maj. John E.)

OSLER, John C. and Chapman,David M. F.

5. DATE OF PUBLICATION (Month and year of publication of document.)

May 1995

6a. NO. OF PAGES (Total containing information. Include Annexes, Appendices, etc.)

34

6b. NO. OF REFS. (Total cited in document.)

5

6. DESCRIPTIVE NOTES (The category of the document, e.g. technical report, technical note or memorandum. If appropriate, enter the type of report, e.g. interim, progress, summary, annual or final. Give the inclusive dates when a specific reporting period is covered.)

DREA Technical Memorandum

8. SPONSORING ACTIVITY (The name of the department project office or laboratory sponsoring the reseach and development. include the address.)

Defence Research Establishment Atlantic
P.O. Box 1012, Dartmouth, N.S. B2Y 3Z7

9a. PROJECT OR GRANT NUMBER (If appropriate, the applicable research and development project or grant number under which the document was written. Please specify whether project or grant.)

DRDM11-12

9b. CONTRACT NUMBER (If appropriate, the applicable number under which the document was written.)

10a. ORIGINATOR'S DOCUMENT NUMBER (The official document number by which the document is identified by the originating activity. This number mrst be unique to this document.)

DREA Technical Memorandum 95/215

10b. OTHER DOCUMENT NUMBERS (Any other numbers which may be assigned this document either by the originator or by the sponsor.)

11. DOCUMENT AVAILABILITY (Any limitations on further dissemination of the document, other than those imposed by security classification)

(X) Unlimited distribution
( ) Distribution limited to defence departments and defence contractors; further distribution only as approved
( ) Distribution limited to defence departments and Canadian defence contractors; further distribution only as approved
( ) Distribution limited to government departments and agencies; futher distribution only as approved
( ) Distribution limited to defence departments; further distribution only as approved
( ) Other (please specify):

12. DOCUMENT ANNOUNCEMENT (Any limitation to the bibliographic annoucement of this document. This will normally correspond to the Document Availability (11). However, where futher distribution (beyond the audience specified in 11) is possible, a wider announcement audience may be selected.)

Full Unlimited

13. ABSTRACT (a brief and factual summary of the document. It may also appear elsewhere in the body of the document itself. It is highly desirable that the abstract of classified documents be unclassified. Each paragraph of the abstract shall begin with an indication of the security classification of the information in the paragraph (unless the document itself is unclassified) represented as (S), (C), (R), or (U). It is not necessary to include here abstracts in both official languages unless the text is bilingual).

The Defence Research Establishment Atlantic moving coil projector (MCP) generates acoustic power at low frequencies (below 250 Hz) by displacing water with two pistons which oscillate in phase. The source level of the MCP must be continually monitored because it varies in accordance with operating state of the projector. Source level as a function of time may be determined by combining measurements of the acceleration of the forward and aft pistons in an appropriate manner. This document establishes the methodology to use in this process by comparing at-sea measured transmission loss of CW signals to theoretical calculations. This comparison reveals that corrections are required to the source level derived from the MCP accelerometers at the higher end of its frequency range.

14. KEYWORDS, DESCRIPTORS or IDENTIFIERS (technically meaningful terms or short phrases that characterize a document and could be helpful in cataloguing the document. They should be selected so that no security classification is required. Identifiers, such as equipment model designation, trade name, military project code name, geographic location may also be included. If possible keywords should be selected from a published thesaurus. e.g. Thesaurus of Engineering and Scientific Terms (TEST) and that thesaurus-identified. If it not possible to select indexing terms which are Unclassified, the classification of each should be indicated as with the title).

acoustic propagation
underwater acoustics
bulk acoustic wave devices
sound transducers
extremely low frequencies
acoustic measurement
moving coil projector
sound pressure
phase angle
acoustic stability